

# Investigating Proto-Planetary Nebulae through Angular Differential Imaging

Rebecca E. Rattray, Dr. Toshiya Ueta

University of Denver



## Background Information

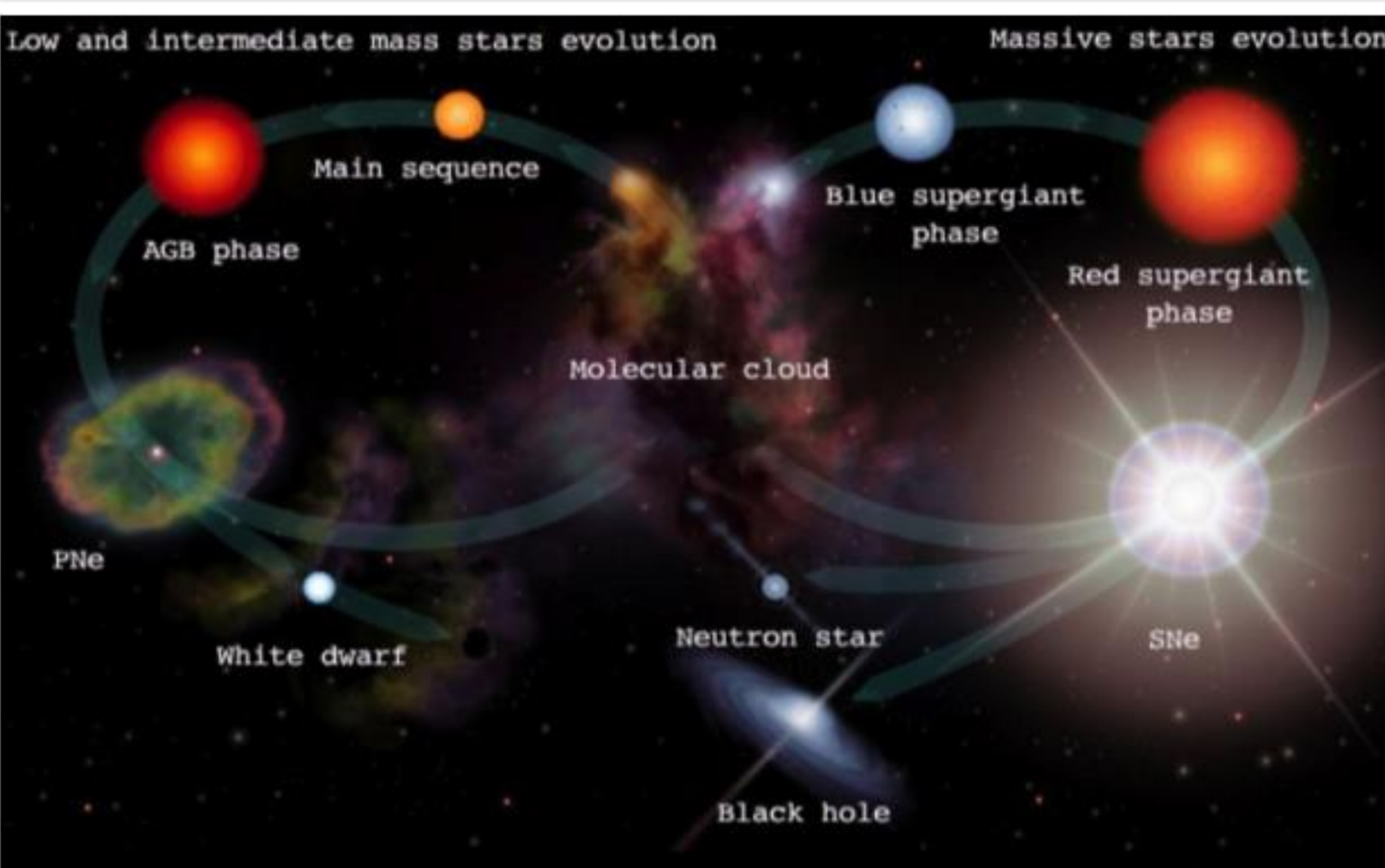


Figure 1: A diagram showing the evolutionary track of stars. The PPN phase is between the AGB phase and the PN phase.

Proto-planetary nebulae (PPNs) are stars between the asymptotic giant branch phase and the planetary nebula phase.<sup>1,2</sup> They evolve over a very short time period (~1000 years) which means we see them rarely in the sky, so they have not been extensively studied. Studying the proto-planetary nebula stage of a star's life sheds light on the critical mass-loss mechanism that leads to the morphological change from spherically symmetric to axisymmetric circumstellar material. However, when studying material very faint in reflection so close to a star, the brightness of the star itself becomes prohibitive. Therefore, in order to study the circumstellar material more effectively, it is necessary to block out the central star.<sup>3</sup>

## Angular Differential Imaging

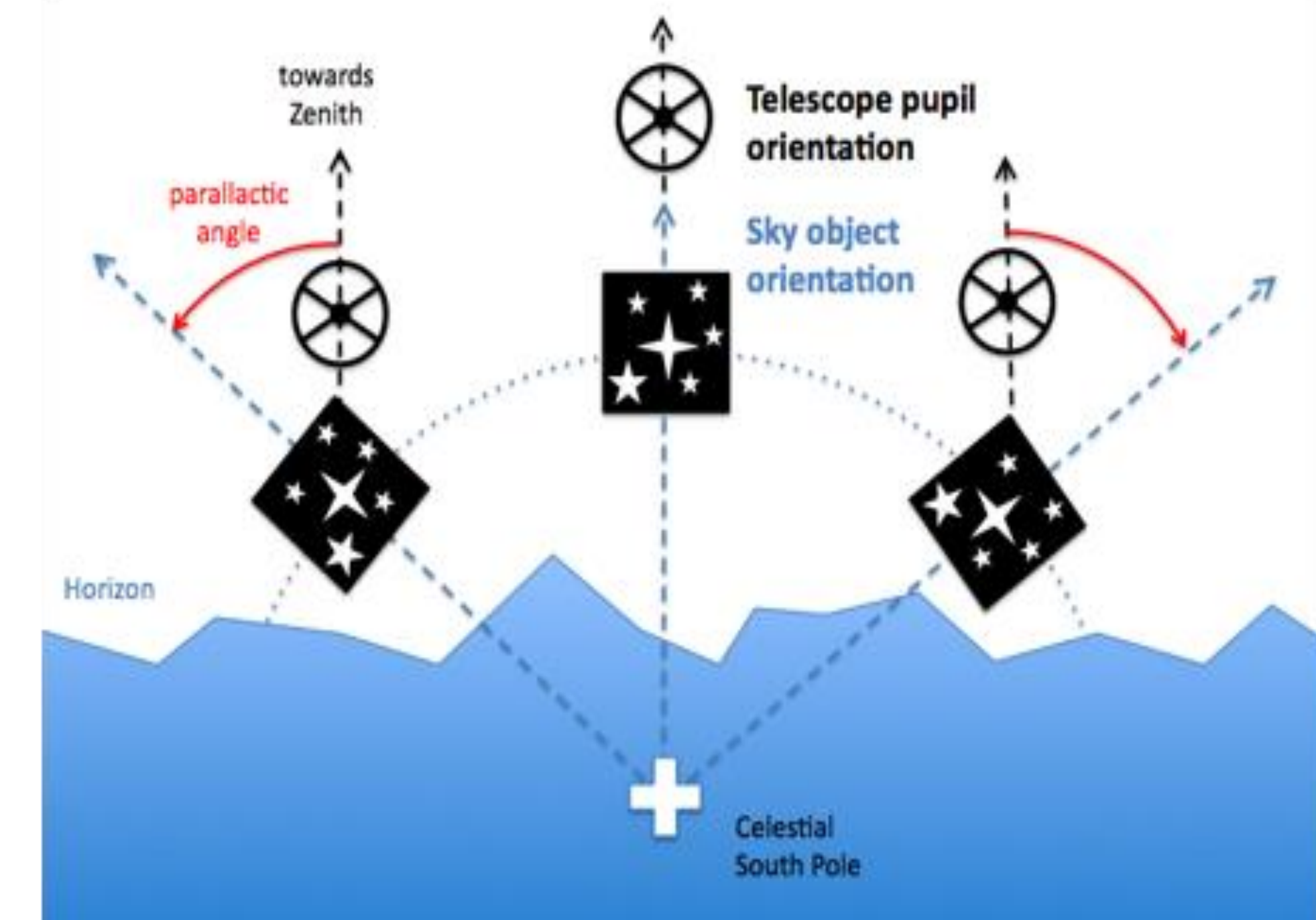


Figure 2: A diagram of the orientation of a telescope using ADI.<sup>4</sup>

The method of Angular Differential Imaging (ADI), used in this research, takes advantage of altitude-azimuth telescopes by turning off the image rotator and allowing a series of images to be taken in which the sky rotates with respect to the instrument frame of reference. This creates a better characterization of the point-spread-function (PSF) of the central star. ADI has successfully been used to verify extrasolar planets, but this is one of the first attempts at adopting ADI as opposed to point sources. In this study, ADI techniques were applied to PPN observations to better study the most recent mass-loss histories of PPNs.

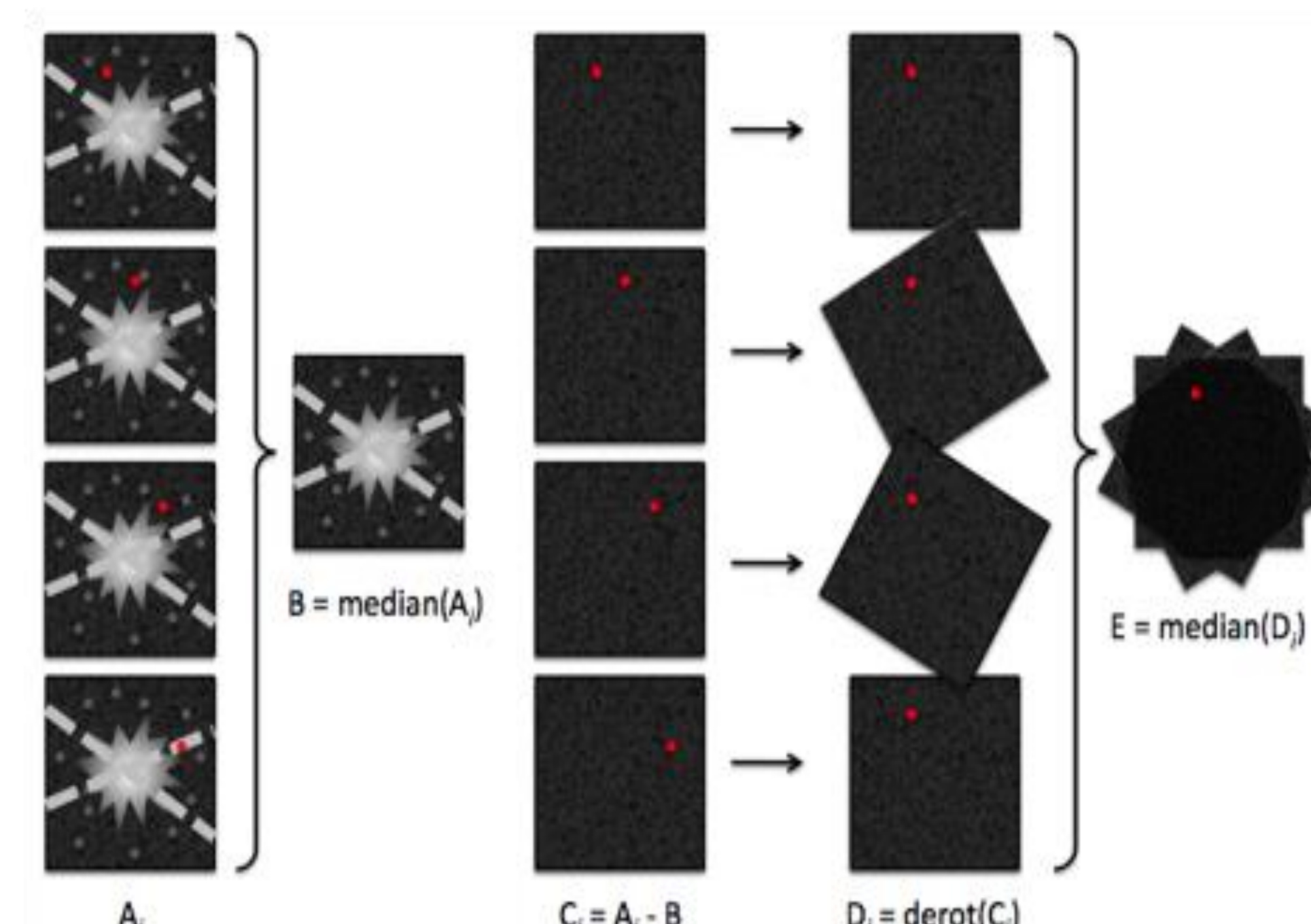


Figure 3: A diagram illustrating how ADI is used to detect a point source (extrasolar planets). Column A shows the raw data, where the red dot is the extrasolar planet. Column B shows the median (which characterizes the PSF). In column C, the PSF has been subtracted from each image. In columns D and E, each image is rotated by its parallactic angle, and then the frames are medianed.<sup>4</sup>

## Data

Data for this study were taken at the Near Infrared Coronagraphic Imager (NICI) at Gemini South between March and September 2012. Data were obtained for 12 PPNs. Some of the PPNs were not imaged sufficiently for effective PSF subtraction; as a result, PSF subtraction was performed for only 6 PPNs: HD179821, IRAS08143-4406, IRAS07134+1005, IRAS08005-2356, IRAS11385-5517, and IRAS12175-5338. Due to the low contrast of the objects studied, this research truly pushed the boundaries of ADI methods.



Figure 4: Picture of the Gemini South 8.1-m telescope

## Methods

Data reduction was done based on the custom reduction codes made by Nelson Zarate<sup>5</sup> and Neil Zimmerman.<sup>6</sup> The codes use ADI techniques with the Locally Optimized Combination of Images algorithm (LOCI),<sup>7</sup> and the Karhunen-Loeve Image Projection algorithm (KLIP).<sup>8</sup> These algorithms are based on the premise that the detector pixels look at the sky most of the time and occasionally at the object in question (i.e., a companion point source) so that the sky emission is recovered for all the detector pixels.

For our cases, however, the object in question is an extended circumstellar shell. Therefore, many detector pixels (especially those close to the central star within the extent of the shell) see the shell most of the time, unless one observes the object for a wide range of parallactic angles. Unfortunately, this was not part of the observational design, and our data were not optimized for these algorithms to work to properly to subtract the PSF of the central star. Instead, we resorted to employ a more basic PSF subtraction technique using a cleaner PSF constructed from data taken with ADI methods for a source without a shell.

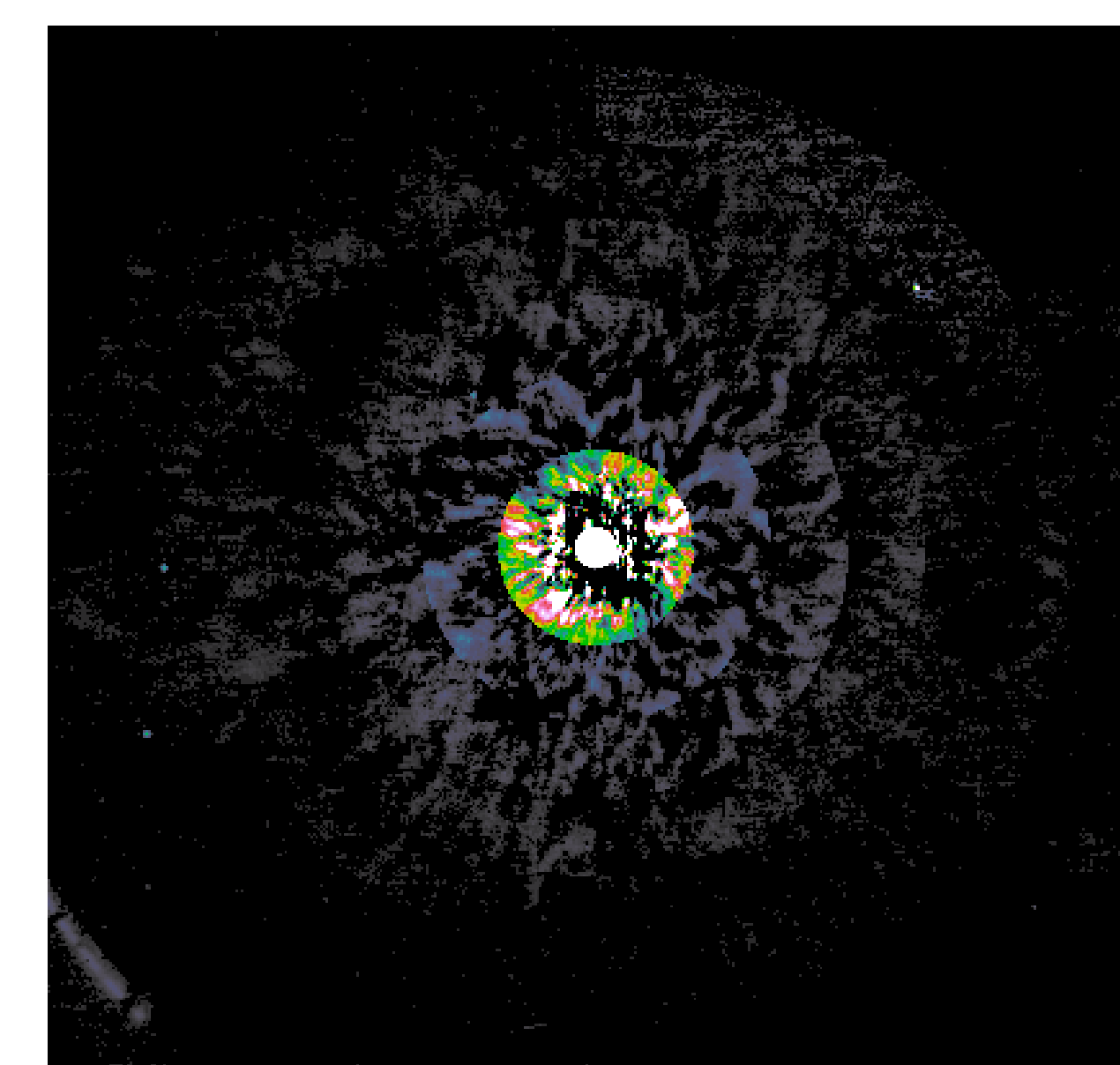


Figure 5: Reduced data using the LOCI method, showing the self-subtraction of the extended emission.

## Results and Final Images

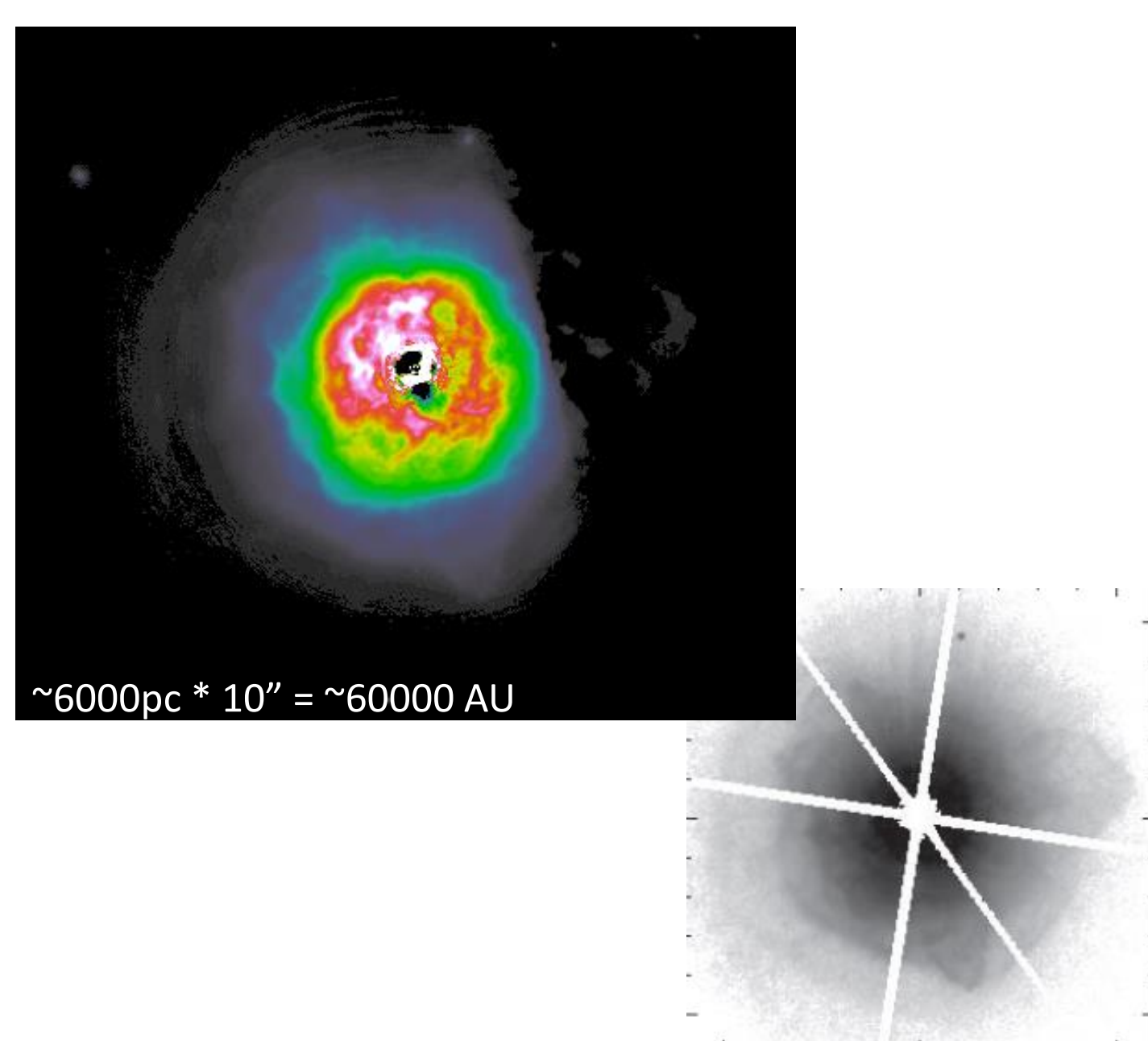


Figure 6: HD179821. Top, new PSF subtracted image, 18"×18". Bottom, Ferguson and Ueta 2010 (12"×12").<sup>9</sup> Previous studies showed concentric arcs in the circumstellar material. Our new image shows much greater detail of the material closest in to the central star.

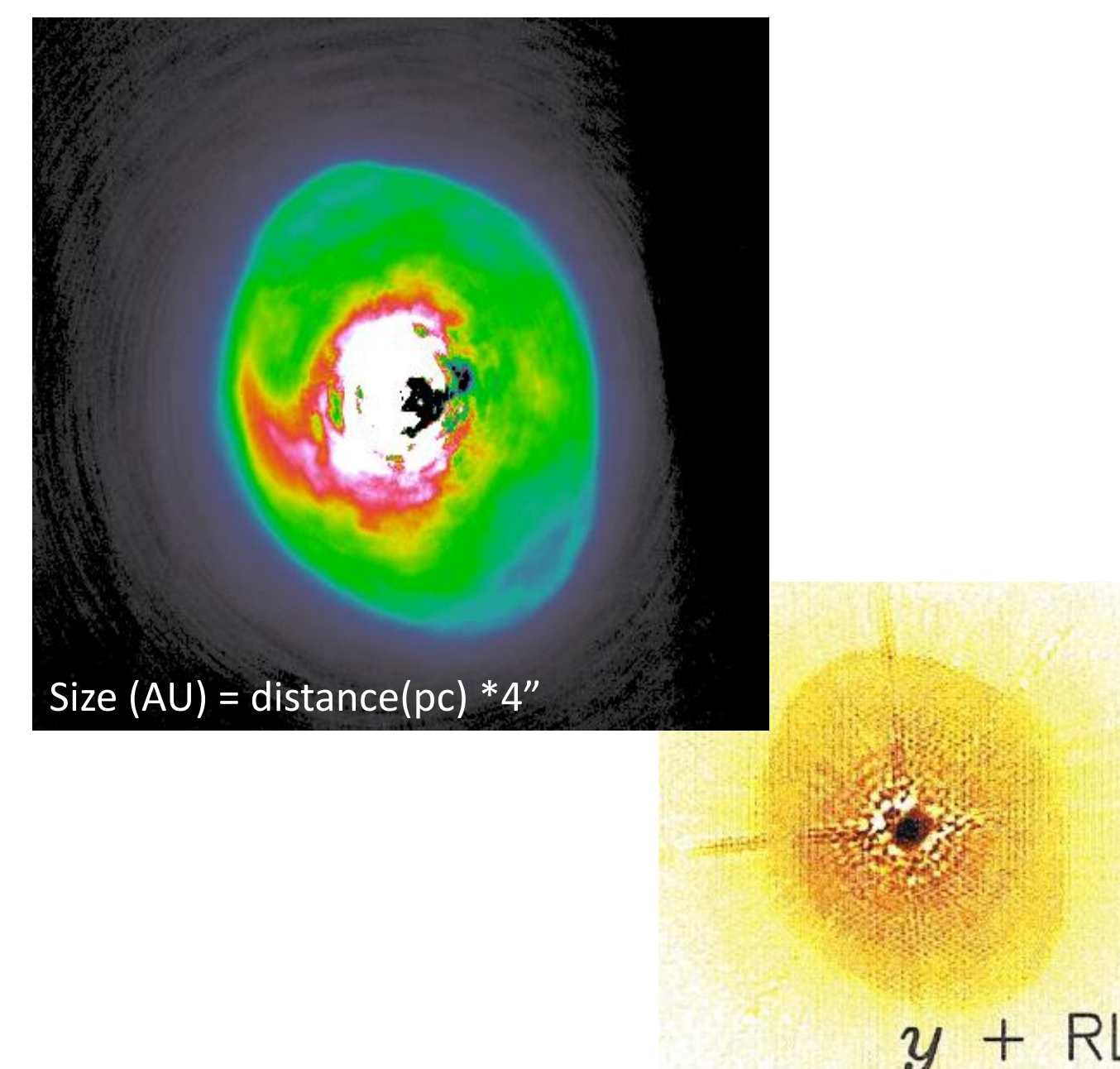


Figure 7: IRAS07134+1005. Top, new PSF subtracted image, 7.7"×7.4". Bottom, from Ueta et al 2000 (6"×6").<sup>10</sup> The general oval shape of the shell is seen in previous images, but our new image shows more detail on the eastern structure.

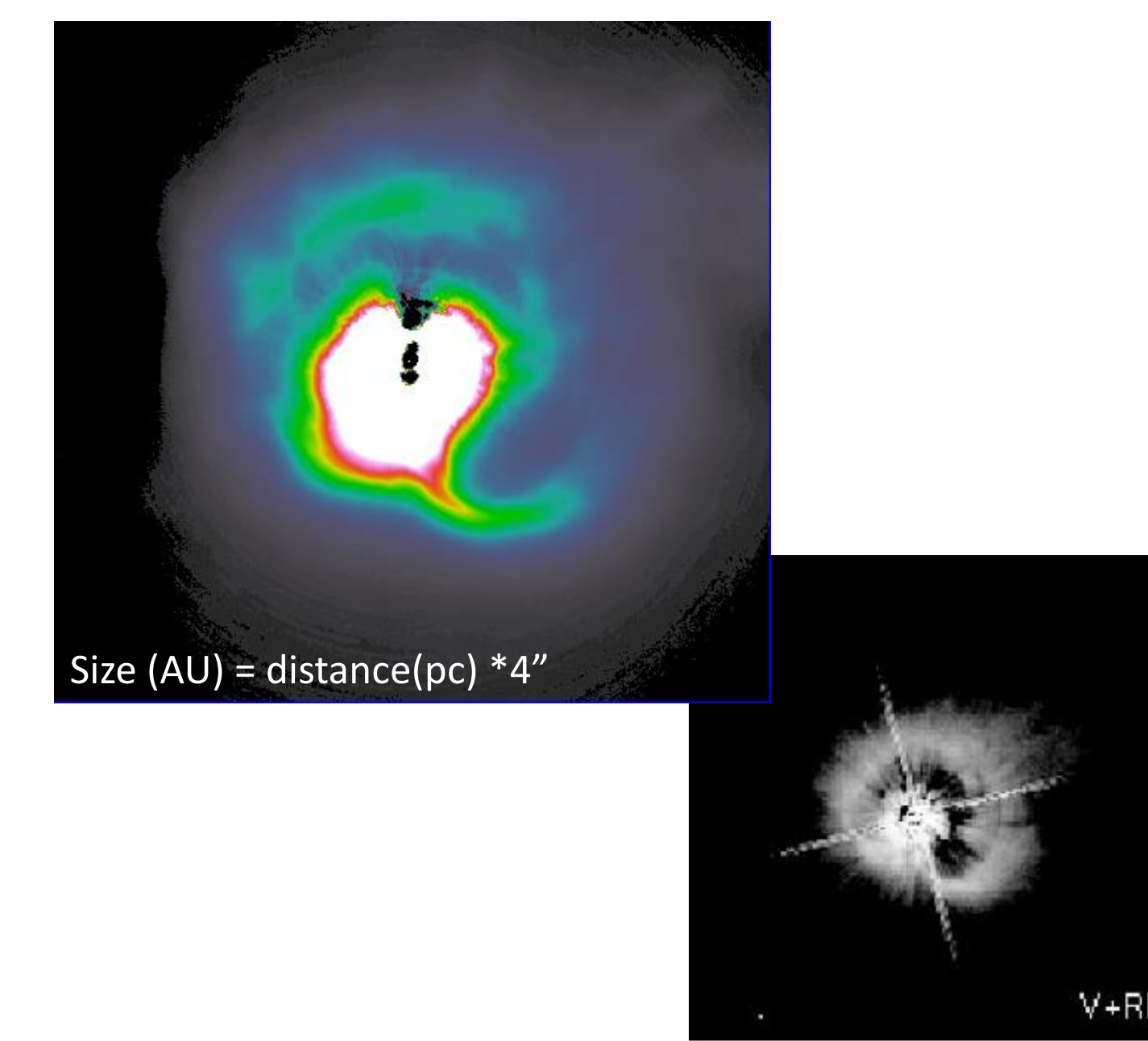


Figure 8: IRAS11385-5517. Top, new PSF subtracted image, 7.7"×7.4". Bottom, from Siodmiak et al 2008 (11.75"×11.75").<sup>12</sup> The general pinwheel structure is shown in previous images. Our new image shows the northern structure and the southern pinwheel arm more clearly than past images.

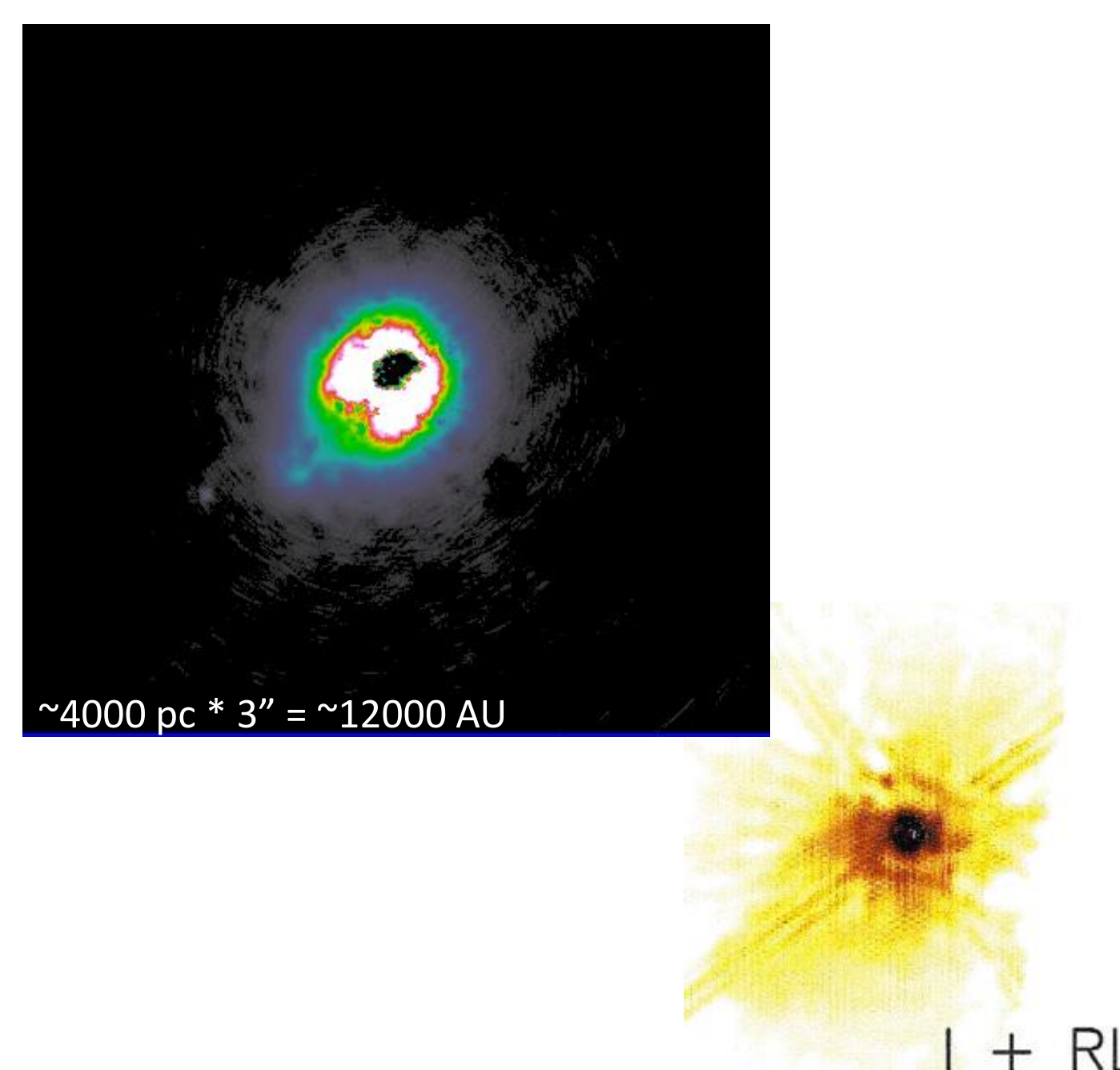


Figure 9: IRAS08005-2356. Top, new PSF subtracted image, 7.7"×7.4". Bottom, from Ueta et al 2000 (4"×3").<sup>10</sup> This PPN was previously known to have a bipolar structure from SE to NW. One of the lobes is shown more clearly in our new image.

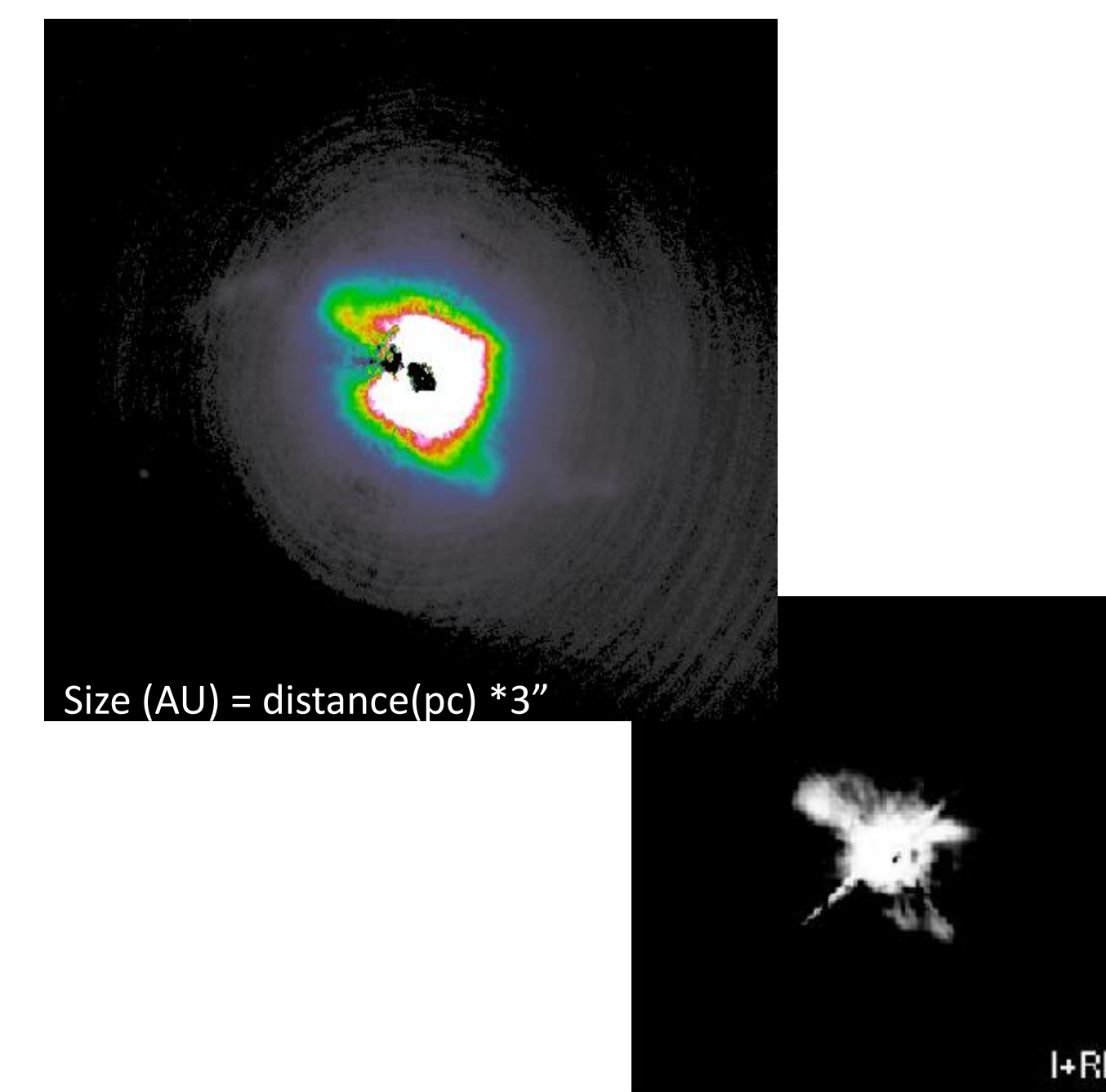


Figure 10: IRAS12175-5338. Top, new PSF subtracted image, 7.7"×7.4". Bottom, from Siodmiak et al 2008 (7.15"×7.15").<sup>12</sup> The bipolar nature of this PPN was already known, but our new image shows much greater detail on the pinwheel arms of the circumstellar material.

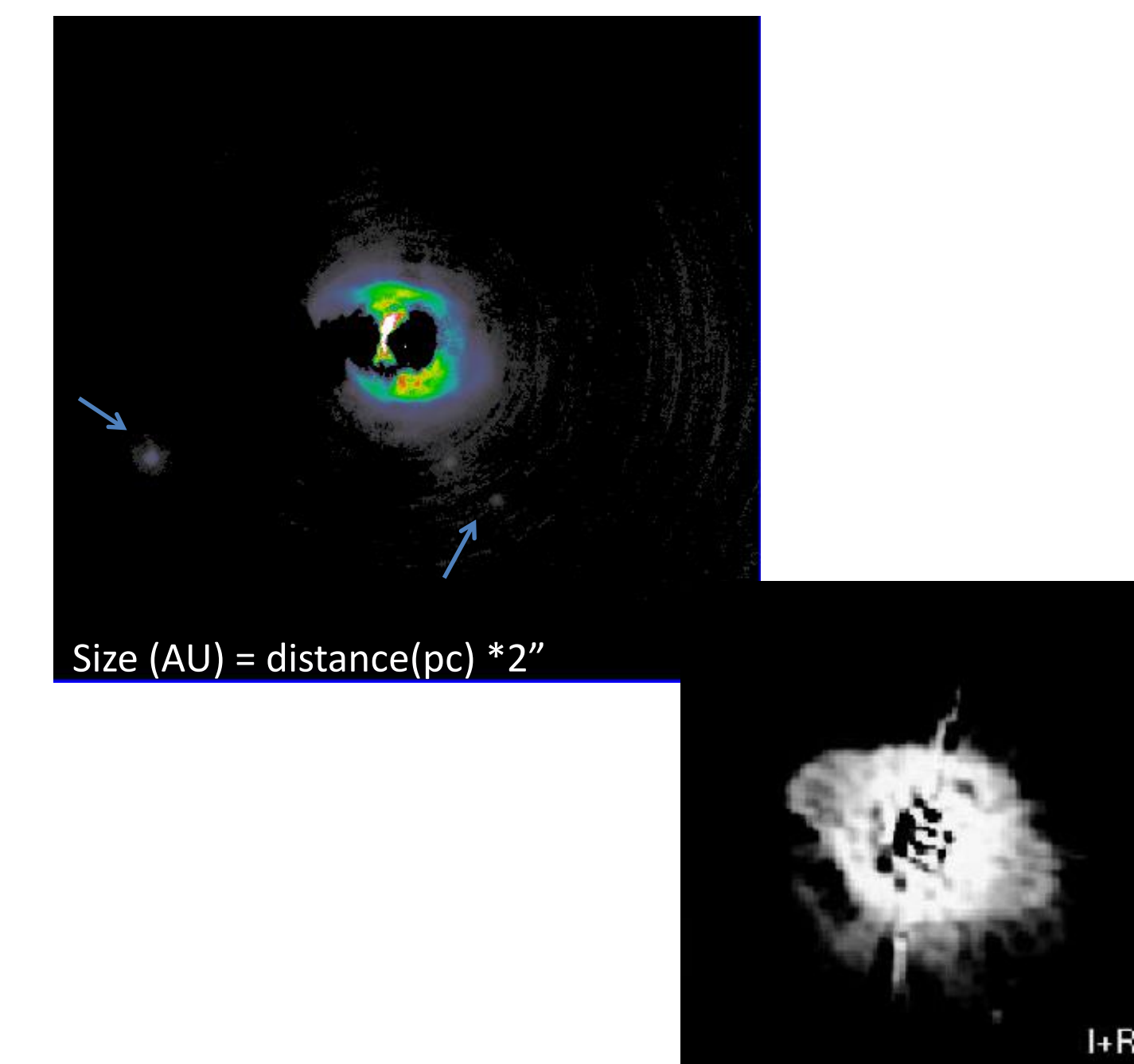


Figure 11: IRAS08143-4406. Top, new PSF subtracted image, 7.7"×7.4". Bottom, from Siodmiak et al 2008 (3.6"×3.6").<sup>12</sup> Previous image shows the elliptical structure of this PPN with lobes pointing to the east and west. Our new image verifies previous discoveries, and shows the presence of two point sources that may be companions.

## Acknowledgments

We would like to acknowledge the University of Denver Department of Physics and Astronomy, as well as Nelson Zarate and Neil Zimmerman for providing code we used in our data reduction process.

## References

1. Kwok, S. 1993. ARA&A, 31:63-92
2. Van Winckel, H. 2003. ARA&A, 41:391
3. Ueta et al. 2005. ApJ, 129:1625-1641
4. Thalmann, Christian. "A Short Introduction to Angular Differential Imaging." <http://www.mpa.de/homes/thalmann/adi.htm>.
5. Zarate et al. 2010. Astronomical Data Analysis Software and Systems XIX. 434:481
6. Zimmerman et al. 2010. ApJ, 709:733-740
7. Lafreniere, D et al. 2007. ApJ, 660:770-780
8. Soummer et al. 2012. ApJ Letters,
9. Ferguson and Ueta, 2010. ApJ, 711:613-618. Distance ≈ 6kpc.
10. Ueta and Meixner, 2000. ApJ, 528:861-884
11. Klochkova and Chentsov, 2004. Astronomy Reports, 48:4. Distance ≈ 4kpc.
12. Siódmiak et al. 2008. ApJ, 677:382-400